EUROGRAPHICS Workshop on Graphics and Cultural Heritage (2022)
R. Pintus and F. Ponchio (Editors)

Short Paper

Lithic Feature Identification in 3D based on Discrete Morse Theory

J.P. Bullenkamp, F. Linsel and H. Mara

Martin-Luther-University of Halle-Wittenberg, Institute of Computer Science, AG eHumanities, FCGLab

Abstract

Neanderthals and our human ancestors have coexisted for a large period of time sharing many things in common including the production of tools, which are among the few remaining artefacts providing a possible insight into the different paths of evolvement and extinction. These earliest tools were made of stone using different strategies to reduce a rather round stone to a sharp tool for slicing, scraping, piercing or chopping. The type of strategy is assumed to be correlated either with our ancestors or the Neanderthals. Recent research uses computational methods to analyse shapes of lithic artefacts using Geometric MorphoMetrics (GMM) as known in anthropology. As the main criteria for determining a production strategy are morphologic measures like shape, size, roughness of convex ridges and concave scars, we propose a new method based on discrete Morse theory for surface segmentation to enable GMM analysis in future work. We show the theoretical concepts for the proposed segmentation, which have been applied to a dataset being available via Open Access. For validation we have created a statistically significant subset of segmented simple and complex lithic tools, which have been manually segmented by an expert as ground truth. We finally show results of our experiments on this real dataset.

CCS Concepts

• ***Applied computing*** → ***Archaeology;*** • ***Theory of computation*** → ***Computational geometry;***

1. Introduction

In the early stone ages, the name-giving stone tools are one of the central object classes which give us insights into the habits of early humans. All human species, from the *H. habilis* over the *H. erectus* finally to the Neanderthals and anatomically modern humans (AMHs), have used at one point stone tools to cut, scrape or pierce other objects. Due to their resilience and endurance, stone tools are commonly preserved in the archaeological record and give us an opportunity to investigate their variety accurately.

For manufacturing stone tools, multiple hammerstones or antlers, sometimes anvils and one nodule of raw material are needed. With hammering on the nodule, pieces are flaking from its surface and leaving negative imprints, so-called *scars* behind, which are enclosed by *ridges*. While hammering, the scar pattern increases in its complexity and results in an artefact as in Figure 1. For the analysis of stone tools, each scar represents one hit and gives a testimony of one action. This clear relation between an object and one production step is easily observable and nearly unique for seeing ancient action so clearly. Segmentating and analysing scars of stone artefacts are central questions for understanding Palaeolithic people and will give us new insight into the concept behind the applied knapping technique.

Due to the high demand for analytical approaches, the publications of Artifact GeoMorph Toolbox3-D (AGMT3-D) by [HG18] and Artifact3-D software by [GMD*22] were created to add new possibilities for analysing 3D models of stone artefacts. Even the use of neural networks to simulate knapping was published by [OFRMT21]. One of the underrepresented and underinvestigated aspects is still the question of the segmentation of scars. Up to now, there is only one article which concentrates on the quantitative analysis of drawn artefacts and their scars [GSF22] and only one other paper by [RGSW14] is addressing this problem for 3D models.

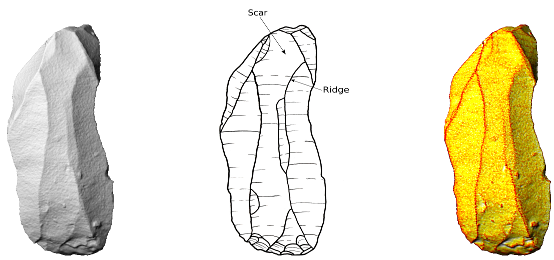

(a) (b) (c)

Figure 1: *Images of the artefact 31 (a) orthographic image; (b) drawing of artefact; (c) MSII-curvature mapped as function value.*

In this paper, we want to present an approach to segment lithic artefacts manufactured by AMHs, which belong to the Proto Aurignacian (42 - 37 ka cal BP). We will introduce a discrete Morse theory based approach on MSII curvature values [MK13] to get ridges, segment the scars and compare our segmentation with manually annotated ground truths.

DOI: 10.2312/gch.20221224

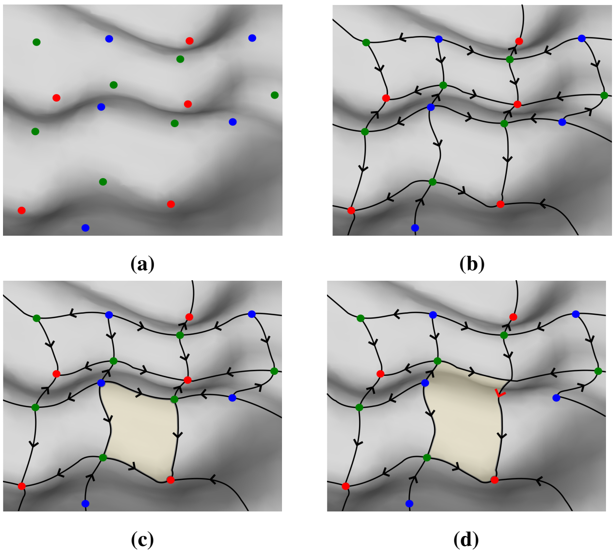

Figure 2: *Surface with the height as Morse function: (a) critical points indicated in red (minima), green (saddle) and blue (maxima); (b) MS complex with separatrices; (c) Morse cell in a MS complex; (d) enlarged Morse cell in a simplified MS complex*

2. Morse Theory Background

In the following, we explain the most important terms of Morse theory and topology that we will use for our segmentation method. Morse theory is a powerful tool in mathematics to calculate the topology of a geometric object from just looking at a scalar function on it, which we will transfer to a segmentation method. Although the concepts work in a more general setting as well, for our purposes it is sufficient to look at a scalar function $f: M \to \mathbb{R}$ on a 2D manifold M. They can be transferred to simplicial complexes - triangular meshes - which is then referred to as discrete Morse theory and builds the theoretical foundation for our segmentation method on a 3D mesh with curvature values as scalar function. For a general overview on discrete Morse theory, we refer to [For01].

2.1. Morse-Smale Complex

The scalar function f is called *Morse function* and we call a point p *critical point*, if the gradient of f is zero at p. In 2D those points are either maxima, saddles or minima and Figure 2 (a) shows how those critical points on a surface equipped with an height function f can look like.

Integral lines, that always follow the gradient of the Morse function, start and end at critical points and we call an integral line *separatrix*, if it is between a maximum and a saddle or a saddle and a minimum (Figure 2 (b)). The separatrices give us neighborhood relations between critical points and their skeleton subdivides the whole surface into different cells, where the Morse function f flows monotonically. These segmented cells are called *Morse cells* and have the separatrices as boundaries as shown in Figure 2 (c). A *Morse-Smale complex* (MS complex) is defined by the critical points and the separatrices connecting them and represents the topology of the whole manifold in a reduced form.

2.2. Persistence

The Morse functions f we will usually deal with, often have a lot of local extrema and thereby produce a large number of topological features, that are induced by noise. A maximum-saddle or saddle-minimum connection can be cancelled in a topologically consistent way by reversing the flow along their separatrix if there is only one separatrix connecting them. This allows to simplify the MS complex to contain only the most dominant topological features.

The importance of a topological feature can be measured using *persistence* as introduced by [ELZ00]. For each saddle s the persistence p_s is the distance to the closest connected extremum e regarding the function values

$$p_s = \min_{e \in \{Extrema\}} (|f(e) - f(s)|) \quad (1)$$

Each cancellation results in a new simplified MS complex with reconnected separatrices and without the two critical points as can be seen in Figure 2 (d). Cancelling all pairs of critical points up to a persistence p then results in a simplified MS complex with enlarged Morse cells.

2.3. Discrete Morse Theory

We interpret a 3D mesh as simplicial complex by defining the vertices as $0-$*simplices*, edges as $1-$*simplices* and faces as $2-$*simplices*. A scalar function on the vertices can be extended to higher simplices such that it defines a discrete Morse function on the simplicial complex and allows to calculate a combinatorial gradient as described in [RWS11]. A detailed overview on discrete Morse theory algorithms and applications can be found in [DFFIM15].

We then have a MS complex on the simplicial complex which can be simplified up to a certain persistence as in the smooth case. Further, we can still define Morse cells to contain all vertices that form a connected component enclosed by separatrices.

3. Method

Our goal is to segment scars of lithic artefacts, which are separated by ridges. The method we used is inspired by [RGSW14] who try to extract the ridges using maximal curvature values and then use a randomly seeded oversegmentation to merge cells together based on a geodesic distance that penalizes crossing ridges.

We replace the ridge detection with persistent separatrices 3.1 and the initial clustering with Morse cells from a noise reduced, simplified MS complex 3.2 and then merge those cells 3.3. The choice of Morse function should meet its purpose, so we chose the MSII curvature values from [MK13], as these curvature values give us a robust detection for ridges.

3.1. Ridge Extraction

Ridge extraction plays a crucial role for getting a good segmentation result. Since the separatrices between critical simplices represent extremal lines, we will use them to get thin and connected ridges. Therefore, we need to introduce a measure defining the importance of a separatrix.

[WG09] have defined a *separatrix persistence* p_{sep} by taking the distance of the points on the separatrix *sep* to the closest other extremum of the saddle point. So for points on a maximum-saddle separatrix, the distance to the closest minimum of the saddle point is taken and for a minimum-saddle separatrix, the closest maximum of the saddle is taken. Since we are only interested in ridges, we do not want to penalize ridges that do not have a larger distance to the next minimum and hence we choose the average Morse function value along the points of a separatrix as importance measure

$$p_{sep} = \frac{1}{|sep|} \sum_{x \in sep} f(x) \tag{2}$$

The advantage over a simple thresholding approach for example is that we can have long separatrices, where the function value drops below a threshold for some parts, which are still included when taking the separatrix persistence.

In practice we will simplify the MS complex to a minimal complex as described in 2.2 - only containing one maximum and minimum each and no separatrices anymore - and calculate the separatrix persistence for all separatrices that are cancelled in the process. Therefore, we have short separatrices of the original MS complex, as well as longer separatrices in the simplified MS complexes and can get ridges of various lengths that can also partially overlap.

Similar to common Canny edge detectors, we use a double threshold $[p^s_{sep}, p^w_{sep}]$ with $p^s_{sep} > p^w_{sep}$ on the separatrices, to get strong (p^s_{sep}) and weak (p^w_{sep}) ridges and include the weak ridges to the output, if they are adjacent to a strong ridge.

3.2. Oversegmentation

Next we need a segmentation of the whole object that will oversegment each scar and we would like it to not cross the calculated ridges from the previous step. The initial MS complex gives us a heavy oversegmentation by taking all Morse cells and we also never cross any of the calculated ridges, as the ridge separatrices always form the boundaries of the initial Morse cells.

To reduce the computation time in the next step, we can also take a slightly simplified MS complex and its corresponding Morse cells as oversegmentation. As described for the smooth case in 2.2 we take a persistence parameter and cancel pairs of critical points below that persistence to enlarge the Morse cells. The calculated ridges are usually not crossed, as they are not induced by noise.

3.3. Merging

Now we can create a weighted adjacency graph of our oversegmentation with Morse cells. Therefore, we need to define the weight between two Morse cells M_i and M_j: Since our detected ridges originate in separatrices and the boundaries of our Morse cells are separatrices as well, we can take the percentage of ridge points along the boundary ∂_{ij} as weight.

We can now merge and update cells of the graph until we reach a threshold, meaning that there are no more adjacent cells with a sufficiently small percentage of ridge points along their boundary. This results in a segmentation of the scars that follows the ridges and can bridge smaller gaps in the ridges.

4. Data

As a case study, we selected stone artefacts from the *Grotta di Fumane* in north-eastern Italy. Thanks to an open-data publication [FP22b], we were able to explore the precision of our method. Out of the 732 artefacts, we selected a set of 30 as ground truths, which we manually segmented using Meshlab's paintbrush tool [CCC*08], to find artefacts with either a complex or simple scar pattern to test the limits of our approach. The same dataset was formally analysed with AGMT3-D [FP22a] and will hence serve as a comparable benchmark dataset. In our study we will focus on artefacts from the layers A1 and A2, which is dated from 41.2-40.4 ka cal BP [HBP*09].

5. Evaluation

To evaluate the correctness of a calculated segmentation with labels L_C, we need to determine which points have been classified correctly based on the ground truth segmentation with labels L_G. Hence, we calculate the *intersection of union* (IoU) for each ground truth label l_g with each of our calculated labels l_c. We then pair up labels, if the calculated label for which the ground truth label has its maximal IoU also has the ground truth label as maximal IoU, so

$$l_g \hat{=} l_c \;\Leftrightarrow\; \max_{l \in L_C}(IoU(l_g, l)) = l_c \text{ and } \max_{l \in L_G}(IoU(l_c, l)) = l_g \tag{3}$$

This guarantees, that neither taking only one label nor taking a very fine segmentation result in high scores. Then we can get the correctness of our segmentation by adding up the intersections of each pair of correctly classified labels and dividing by the total number n of vertices of the mesh

$$Score = \frac{1}{n} \sum_{l_c \hat{=} l_g} |l_c \cap l_g| \tag{4}$$

The *Score* thereby gives us a percentage of correctly labelled vertices.

6. Results

We implemented our segmentation pipeline in Python and evaluated it for a wide variety of parameters on each of the 30 artefacts. The parameters to be chosen are the double threshold for ridge detection $[p^s_{sep}, p^w_{sep}]$ and a merging parameter giving a minimum percentage of ridge points on a boundary between two cells. These two parameters are dependent on each other, as lower ridge detection thresholds can be compensated by a higher merging parameter. Testing with many parameters and evaluating all of them, allows us to include an automated parameter determination in future.

In Figure 3 we can see the interim results of our Morse-theoretic pipeline: We first get the ridges (a), oversegment with Morse cells (b) and then merge according to the ridges (c). Compared to the manually annotated ground truth (d) we reach a score of 93.5% on this artefact. Averaged over the 30 artefacts we manually annotated, our method has a score of **92.2%** for the best parameter combination for each artefact. For simple artefacts with clear ridges our algorithm classifies up to 97.1% (best result) of the vertices correctly Figure 4 (c), while more difficult artefacts with large uneven areas like Figure 4 (d) only reach 83.4% due to the incorrectly classified points on the coarse part.

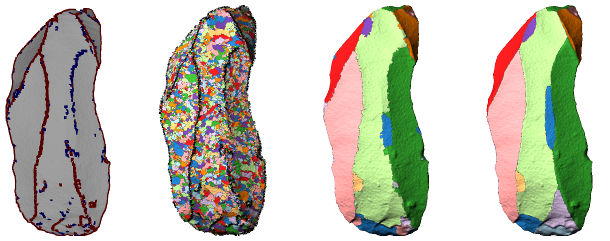

(a) *Ridges* **(b)** *Oversegmentation* **(c)** *Result* **(d)** *Ground truth*

Figure 3: *(a) double thresholded ridges: strong ridges (red), weak ridges (blue); (b) oversegmentation from a slightly simplified MS complex; (c) result after merging; (d) ground truth segmentation*

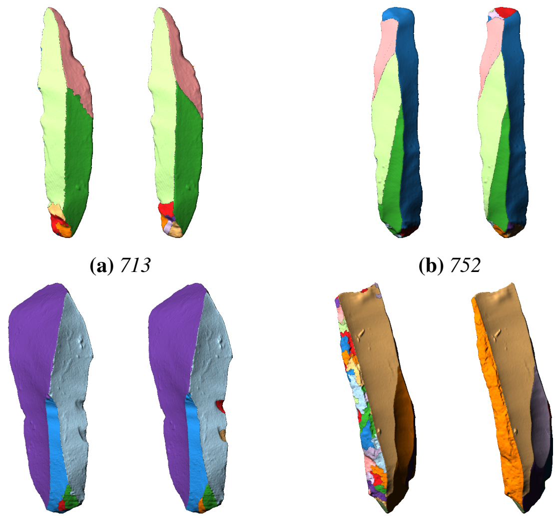

(a) *713* **(b)** *752* **(c)** *4501* **(d)** *700*

Figure 4: *(a)-(d): different results (left) with ground truths (right)*

The two main challenges for our segmentation method, are weak scars and rough areas. Weak scars often do not have enough ridges that we can detect in order to not be merged into a surrounding scar. Examples can be seen in Figure 4 (c) where the two smaller scars at the dents do not have enough ridges to be detected as well as the smaller scars in Figure 3 (d) at the bottom and partially in the middle. Rough and uneven areas that were not created by knapping on the other side will result in too many strong ridges and hence too many small segments on an area that a human will identify as one large segment. Such an example can be seen in Figure 4 (d).

7. Outlook

We presented a segmentation method for scars of lithic artefacts based on discrete Morse theory. Since especially the ridge detection determines the success of a segmentation, we plan to improve this part. Further, we will work on automating the parameter choices and compare our method with the Artifact3-D software which uses the algorithm of [RGSW14] and also depends on four tuneable parameters. Scar property analysis will be the next step, as a good segmentation allows to extract spatial attributes of each scar like area, curvature and slope enabling classification of lithic artefacts.

References

[CCC*08] Cignoni P., Callieri M., Corsini M., Dellepiane M., Ganovelli F., Ranzuglia G.: MeshLab: an Open-Source Mesh Processing Tool. In *Eurographics Italian Chapter Conference* (2008), pp. 129–136. doi:10.2312/LocalChapterEvents/ItalChap/ItalianChapConf2008/129-136. 3

[DFFIM15] De Floriani L., Fugacci U., Iuricich F., Magillo P.: Morse complexes for shape segmentation and homological analysis: discrete models and algorithms. In *Computer Graphics Forum* (2015), vol. 34, pp. 761–785. doi:10.1111/cgf.12596. 2

[ELZ00] Edelsbrunner H., Letscher D., Zomorodian A.: Topological persistence and simplification. In *Proceedings 41st annual symposium on foundations of computer science* (2000), pp. 454–463. doi:10.1109/SFCS.2000.892133. 2

[For01] Forman R.: A User's Guide To Discrete Morse Theory. *Séminaire Lotharingien de Combinatoire 48* (2001), B48c–35. 2

[FP22a] Falcucci A., Peresani M.: The contribution of integrated 3D model analysis to Protoaurignacian stone tool design. *PLOS ONE 17*, 5 (2022), 1–29. doi:10.1371/journal.pone.0268539. 3

[FP22b] Falcucci A., Peresani M.: The Open Aurignacian Project. Volume 1: Fumane Cave in northeastern Italy, (2022). doi:10.5281/zenodo.6362150. 3

[GMD*22] Grosman L., Muller A., Dag I., Goldgeier H., Harush O., Herzlinger G., Nebenhaus K., Valetta F., Yashuv T., Dick N.: Artifact3-D: New software for accurate, objective and efficient 3D analysis and documentation of archaeological artifacts. *PLOS ONE 17*, 6 (2022), 1–24. doi:10.1371/journal.pone.0268401. 1

[GSF22] Gellis J. J., Smith C. R., Foley R. A.: PyLithics: A Python package for stone tool analysis. *Journal of Open Source Software 7*, 69 (2022), 3738. doi:10.21105/joss.03738. 1

[HBP*09] Higham T., Brock F., Peresani M., Broglio A., Wood R., Douka K.: Problems with radiocarbon dating the Middle to Upper Palaeolithic transition in Italy. *Quaternary Science Reviews 28*, 13 (2009), 1257–1267. doi:10.1016/j.quascirev.2008.12.018. 3

[HG18] Herzlinger G., Grosman L.: AGMT3-D: A software for 3-D landmarks-based geometric morphometric shape analysis of archaeological artifacts. *PLOS ONE 13*, 11 (2018), 1–17. doi:10.1371/journal.pone.0207890. 1

[MK13] Mara H., Krömker S.: Vectorization of 3D-Characters by Integral Invariant Filtering of High-Resolution Triangular Meshes. In *2013 12th International Conference on Document Analysis and Recognition* (2013), pp. 62–66. doi:10.1109/ICDAR.2013.21. 1, 2

[OFRMT21] Orellana Figueroa J. D., Reeves J. S., McPherron S. P., Tennie C.: A proof of concept for machine learning-based virtual knapping using neural networks. *Scientific Reports 11* (2021), 1–12. doi:10.1038/s41598-021-98755-6. 1

[RGSW14] Richardson E., Grosman L., Smilansky U., Werman M.: Extracting Scar and Ridge Features from 3D-scanned Lithic Artifacts. *Archaeology in the Digital Era: 40th Annual Conference of Computer Applications and Quantitative Methods in Archaeology (CAA)* (2014), 83–92. doi:10.1515/9789048519590-010. 1, 2, 4

[RWS11] Robins V., Wood P., Sheppard A.: Theory and Algorithms for Constructing Discrete Morse Complexes from Grayscale Digital Images. *IEEE transactions on pattern analysis and machine intelligence 33* (2011), 1646–1658. doi:10.1109/TPAMI.2011.95. 2

[WG09] Weinkauf T., Günther D.: Separatrix persistence: Extraction of salient edges on surfaces using topological methods. In *Computer Graphics Forum* (2009), vol. 28, pp. 1519–1528. doi:10.1111/j.1467-8659.2009.01528.x. 3